

# Spatial scaling properties of coral reef benthic communities

Ford, Helen; Gove, Jamison M. ; Davies, Andrew; Graham, Nicholas A.J.; Healey, John; Conklin, Eric; Williams, Gareth J.

**Ecography**

*DOI:*
https://doi.org/10.1111/ecog.05331

Published: 01/02/2021

Peer reviewed version

# Spatial scaling properties of coral reef benthic communities

Helen V. Ford[1*], Jamison M. Gove[2], Andrew J. Davies[3], Nicholas A. J. Graham[4], John R. Healey[5], Eric J. Conklin[6], and Gareth J. Williams[1*]

[1]School of Ocean Sciences, Bangor University, Anglesey, LL59 5AB, UK

[2]NOAA Pacific Islands Fisheries Science Centre, Honolulu, HI, USA

[3]Department of Biological Sciences, University of Rhode Island, Kingston, RI, USA

[4]Lancaster Environment Centre, Lancaster University, UK

[5]School of Natural Sciences, Bangor University, Bangor, Gwynedd, LL57 2UW, UK

[6]The Nature Conservancy, 923 Nuuana Avenue, Honolulu, HI, USA

[*]Email: helen.ford@bangor.ac.uk, g.j.williams@bangor.ac.uk, Tel: +44(0)1248 382588

**Keywords:** autocorrelation, benthic ecology, physical drivers, scale, seascape, coral morphology

**Abstract:**

The spatial structure of ecological communities on tropical coral reefs across seascapes and geographies have historically been poorly understood. Here we addressed this for the first time using spatially expansive and thematically resolved benthic community data collected around five uninhabited central Pacific oceanic islands, spanning 6° latitude and 17° longitude. Using towed-diver digital image surveys over ~140 linear km of shallow (8 – 20 m depth) tropical reef, we highlight the autocorrelated nature of coral reef seascapes. Benthic functional groups and hard coral morphologies displayed significant spatial clustering (positive autocorrelation) up to kilometre-scales around all islands, in some instances dominating entire sections of coastline. The scale and strength of these autocorrelation

patterns showed nuances across geographies, but patterns were more similar between islands in closer proximity and of a similar size. For example, crustose coralline algae (CCA) were clustered up to scales of 0.3 km at neighbouring Howland and Baker Islands and macroalgae were spatially clustered at scales up to ~3 km at both neighbouring Kingman Reef and Palmyra Atoll. Of all the functional groups, macroalgae had the highest levels of spatial clustering across geographies at the finest resolution of our data (100 m). There were several cases where the upper scale at which benthic community members showed evidence of spatial clustering correlated highly with the upper scales at which concurrent gradients in physical environmental drivers were spatially clustered. These correlations were stronger for surface wave energy than subsurface temperature (regardless of benthic group) and turf algae and CCA had the closest alignments in scale with wave energy across functional groups and geographies. Our findings suggest such physical drivers not only limit or promote the abundance of various benthic competitors on coral reefs, but also play a key role in governing their spatial scaling properties across the seascape.

## Introduction

Patterns in nature are often highly scale dependent (Levin 1992). Conclusions drawn from observations at one scale may be inconsistent when observing at another scale. Scales of observation in ecology are often chosen for arbitrary, logistical or anthropocentric reasons and may not be appropriate for the target organism, system or process in question (Addicott et al. 1987, Wiens and Milne 1989, Boström et al. 2011). Such mismatches of scale can reduce our predictive capacity of ecosystem dynamics and lead to erroneous extrapolations over larger scales from spatially or temporally limited sampling observations (Hatcher et al. 1987, Schneider 2001). Despite this, observational scales in ecology have generally remained constrained and limit our understanding of the scaling of natural systems (Estes et al. 2018).

By conducting ecological investigations at systematically varied scales, the dynamics of natural systems and how they vary as a function of scale can be properly quantified (Rahbek and Graves 2000, Nash et al. 2014).

Since the 1980's, ecology has benefitted from an advancement of concepts related to ecological pattern and scale, including the idea that biological spatial patterns emerge at characteristic scales in response to their environment (Wiens and Milne 1989, Levin 1992, Schneider 1994). The progression of 'landscape ecology' theory occurred alongside an increased diversity of field techniques, most notably remote sensing technology (Dungan et al. 2002, Wagner and Fortin 2005). These technologies greatly expanded scales of observation and enabled practical implications of landscape ecology to be used in ecosystem management (Lee et al. 2008, De Knegt et al. 2011, Jones et al. 2013). Progression of theory within the marine environment has been slower due to logistical constraints of collecting comparable data across scales (Kenny et al. 2003, Hinchey et al. 2008, D'Urban Jackson et al. 2020), but has nonetheless emerged to form the discipline of 'seascape ecology' (Pittman et al. 2011).

On tropical coral reefs, spatial scales of observation were greatly expanded by the onset of remote sensing technology, permitting their global-scale mapping to a coarse taxonomic resolution (Mumby et al. 1997, Hochberg and Atkinson 2003, Purkis 2018). More recently, *in situ* digital imaging techniques, such as structure-from-motion photogrammetry, have enabled us to study the spatial ecology of coral reef benthic communities at higher taxonomic resolutions (Edwards et al. 2017, Pedersen et al. 2019). Despite these important advances, such data re-introduce the issue of limited sampling extents and previous research has instead tended to focus on comparing spatial patterns across discrete hierarchical scales (Murdoch and Aronson 1999, Williams et al. 2015b). By combining high-resolution digital imagery with towed-diver surveys, recent research has started to reveal the spatial structure of

77 coral reef benthic communities around entire tropical islands (Gove et al. 2015, Aston et al.
78 2019). These data present the opportunity to apply landscape ecological theory and spatial
79 pattern metrics to the marine realm to explore ecological patterns and processes across scales
80 (Wedding et al. 2011).

81 Spatial autocorrelation is a long-standing statistical technique within ecology
82 (Legendre 1993, Cocu et al. 2005) that describes the similarity of a given variable at nearby
83 locations as being greater or less than expected by chance (Fortin et al. 2016). It can be
84 quantified over multiple scales to show how species, habitats and environmental variables are
85 spatially structured. Environmental conditions can be spatially autocorrelated due to several
86 factors, such as climate and geomorphologic processes, which in turn can drive the spatial
87 autocorrelation patterns of ecological communities (Legendre 1993, Gobbi and Brambilla
88 2016).

89 The scale at which spatial autocorrelation is no longer present or changes from being
90 clustered to over-dispersed can indicate a new process acting on biological variables (Zhang
91 and Zhang 2011). Spatial autocorrelation has been used to quantify forest fragmentation
92 (Zhang et al. 2009), optimise sampling protocols for marine macrobenthic invertebrate
93 communities (Hamylton and Barnes 2018) and to relate spatial patterns of insect abundance
94 to environmental gradients (Cocu et al. 2005). On coral reefs, indices of spatial
95 autocorrelation have been used to quantify the spatial patterning of coral bleaching across
96 scales of cm to 100s of m (Levy et al. 2018) and benthic communities up to kilometre-scales
97 around the circumference of a single tropical island (Aston et al. 2019). Despite these recent
98 efforts, our understanding of the patterns of spatial autocorrelation of coral reef communities
99 across scales and geographies remains limited.

100 Here we quantify the spatial scaling properties of tropical benthic communities over
101 ~140 linear km of reef around the circumference of five uninhabited coral reef islands. By

processing thousands of *in situ* benthic images and using *in situ* and modelled environmental data, we employ a spatial metric to quantify the patterning of competing functional groups, hard coral morphologies and their suspected physical drivers across scales. Wave energy and subsurface variations in seawater temperature, indicative of intra-island gradients in upwelling (Gove et al., 2006, Aston et al. 2019), can limit or promote the abundance of different benthic groups around tropical islands, including different morphologies (growth forms) of reef-building corals (Williams et al. 2013, Gove et al. 2015). We therefore expect these physical drivers to play a role in the spatial ecology and spatial scaling of tropical benthic communities. Our study objectives were primarily to test whether the intra-island distributions of benthic communities differed from random and if so, up to what scales. We then asked how consistent these spatial scaling properties were across geographies and to what degree they correlated with the spatial scaling of concurrent gradients in physical drivers. Our study therefore establishes important baselines for the spatial ecology of coral reef benthic communities in a world where escalating human interactions with coral reefs (Norström et al. 2016, Hughes et al. 2017, Williams et al. 2019) are fundamentally altering their biological-environmental relationships (Williams et al. 2015a).

## Methods

### Study sites

Our study system consisted of five U.S.-affiliated coral reef islands and atolls (hereafter referred to as 'islands') spanning 6° latitude and 17° longitude in the central Pacific Ocean (Fig. 1): Jarvis Island, Palmyra Atoll, Kingman Reef (Line Islands Archipelago), Howland Island, and Baker Island (U.S. Phoenix Islands). In 1974, Jarvis, Baker and Howland became U.S. National Wildlife Refuges. Kingman and Palmyra were afforded the same protection in 2001. All five islands were declared part of the Pacific Remote Islands

Marine National Monument in 2009, further affirming their protected status. Throughout their history, these five islands have lacked permanent human populations and represent some of the most remote coral reef ecosystems on the planet. As such, they offer the opportunity to study the ecology and natural variation of coral reefs in the absence of confounding direct local human impacts (Williams et al. 2015, Heenan et al. 2020), within a relatively similar oceanographic and climatic setting (Gove et al. 2013).

**Benthic community digital surveys and spatial processing**

Digital benthic images were collected around the circumference of each island using towed-diver surveys (Kenyon et al. 2006) in March to April 2008 as part of the National Oceanic and Atmospheric Administration's (NOAA) Pacific Island Fisheries Science Center's (PIFSC) Pacific Reef Assessment and Monitoring Program (RAMP). This survey year was chosen for the present study from the biennial/triennial surveys at each island spanning 2001 to the present due to: 1) representing 10 years of recovery potential following the suspected mass coral bleaching in 1998, and 2) being prior to a bleaching event that affected the region in late 2009 to early 2010 (Williams et al. 2010, Vargas-Ángel et al. 2011). As such, this survey year provided the least disturbed benthic community spatial patterns within the time series. Divers manoeuvred a sub-surface instrumented board towed by a surface boat at ~3 km $h^{-1}$ to target the 15 m depth contour around each island. The tow-board was equipped with a downward facing digital SLR camera (Canon EOS 10-D/50-D) and strobes, taking images every 15 s (equating to every ~15 m) from a height of ~1 m above the benthos. The average area of the benthos that each survey image captured using this technique was 10.9 $m^2$ (SE=0.1 $m^2$, n=700) (Kenyon et al. 2006).

Every alternate image was selected for subsequent analyses and images were filtered to only include those within a depth range of 8 – 20 m on the forereef habitat (reef slope

facing the open ocean) of each island to ensure comparability with prior studies in the region (Gove et al. 2015, Williams et al. 2015a, Aston et al. 2019). We used the analysis software CoralNet (Beijbom et al. 2015) to overlay 10 points in a stratified-random design over each photo and identify the benthos below each as either: hard coral (to morphology), macroalgae, soft coral, crustose coralline algae, turf algae, other invertebrates (echinoderm, bivalve, zoanthid, anemone, corallimorph), and bare sand (for detailed descriptions of functional groups and coral morphologies see Supplementary material Appendix 1, Table A1 and A2).

A Global Positioning System (GPS) aboard the boat timestamped to the camera and a SeaBird$^{TM}$ Electronics (SBE) 39 subsurface pressure, temperature-depth recorder on the tow-board, combined with a layback algorithm (Kenyon et al. 2006), allowed each photograph to be georeferenced to the nearest ~3 – 5 m and depth referenced. For the few instances where depth data were missing, we used an interpolation based on inverse distance weighting using the Spatial Analyst tool in ArcGIS (v 10.7.1) and matched the missing depths to interpolated depth data from the same island area from surveys in 2006 and 2010. Each island's circumference was divided into a series of discrete, sequentially numbered grid cells (100 m wide) using a custom Python script (*sensu* Aston et al. 2019, <https://doi.org/10.5281/zenodo.1199350>); the number of grid cells around each island ranged from 77 to 340. Benthic image data were spatially joined to each grid cell and, to be included in further spatial analyses, grid cells had to contain ≥ 4 benthic images (*sensu* Aston et al. 2019). To help satisfy this prerequisite and maximise spatial coverage around each island, for those grid cells with < 4 images we revisited our initial filtering step (where we excluded every alternate image) and re-selected some images for processing. In total, we processed 6022 images across the five islands (Howland, 787; Baker, 838; Jarvis, 1107; Kingman, 1560; Palmyra, 1730) to calculate a mean cover value for each benthic variable per grid cell,

with 77% to 96% of grid cells containing data around the five islands (see Supplementary Material Appendix 1, Table A3).

**Quantifying physical drivers**

We calculated surface wave power using a 3-hr output at 50 km resolution from NOAA's Wave Watch III global model (WWIII; <http://polar.ncep.noaa.gov/waves>). Wave power (W $m^{-1}$) was calculated from significant wave height ($H_s$) and peak period ($T_p$), defined as:

$$WP = \frac{\rho g^2 T_p H_s^2}{64\pi}$$

where $\rho$ is the density of seawater (1024 kg $m^{-3}$) and $g$ is the acceleration of gravity (9.8 m $s^{-2}$). From this output, calculations using an incident wave swath method (*sensu* Aston et al. 2019) estimated the wave power at regularly spaced locations (between on island) around each island, ranging from ~100 – 500 m depending on island size We calculated an integrated 10-yr average (1998 – 2008) in wave energy flux (kW hr $m^{-1}$) for each location and used a 250 m radial buffer around each location to spatially join to the 100 m grid cells, averaging values within cells that contained multiple overlapping buffers.

*In situ* seawater temperature was recorded during each towed-diver survey in 2008 using the SBE39 logger attached to the towboard (10 s sample rate, 0.002 °C accuracy). Despite being a temporal snapshot, these *in situ* temperature data capture long-term intra-island gradients in sub-surface temperature that are indicative of localised upwelling (Gove et al. 2006). Like the benthic and wave data, we spatially joined the subsurface temperature data to each discrete island grid cell and calculated a mean value per cell.

**Spatial statistics and sensitivity analyses**

To quantify changes in the spatial autocorrelation of benthic communities and their physical drivers across scales, we used the Moran's I statistic (Moran 1950) twithin a custom-coded function (Aston et al. 2019) in the R programming language (R Core Team 2019), and which we build upon here to allow the comparison of these patterns across islands. When calculating the Moran's I statistic for hard coral morphologies, we selected the two to three most abundant morphologies at each island. We defined the observed Moran's I value (OMI) as:

$$I = \frac{n}{S_0} \frac{\sum_{i=1}^{n} \sum_{j=1}^{n} w_{i,j}(x_i - \bar{x})(x_j - \bar{x})}{\sum_{i=1}^{n}(x_i - \bar{x})^2}$$

where $n$ is the number of observations, $w_{i,j}$ is the matrix of weights according to the inverse Euclidean distance between observations, $x_i$ is the observed value at location $i$, $x_j$ is the observed value at location $j$, $\bar{x}$ is the mean value and $S_0$ is the sum of spatial weights. The spatial weights are defined as the inverse of the minimum distance, $d_{i,j}$, around the circumference of each island between locations $i$ and $j$, as follows:

$$d_{i,j} = min\big((j - i), (n + i - j)\big)$$

$$w_{i,j} = \frac{1}{d_{i,j}} \; for \; i \neq j, 0 \; otherwise$$

A significant ($p < 0.05$) departure from an OMI value of zero (i.e. away from a random distribution) indicated that the spatial pattern of the variable in question at that scale was highly organised in space. Positive OMI values indicated positive autocorrelation (i.e. spatial clustering), while negative OMI values indicated negative autocorrelation (i.e. over-dispersion). We calculated the Moran's I statistic at the finest spatial resolution of the data (100 m grid cells), and then again in a moving window averaging process at increasing 100-m increments to a maximum scale of 4 km (limited by replication beyond that scale due to island size). Grid cells containing 'no data' (i.e. < four benthic images) were excluded from the moving window averaging process. As spatial patterns in nature can be anisotropic, at

each scale we re-computed the Moran's I statistic and p-value for all possible 100 m grid cell starting locations of the moving window averaging process and iterating in both directions around the circumference of each island. We report the mean, maximum and minimum OMI value for each scale from this process and the scale at which the upper bound of p exceeded 0.05 (i.e. did not differ significantly from a random spatial distribution).

As the number of grid cells with 'no data' varied across islands (Fig.1), we performed a series of sensitivity analyses to quantify the possible impact this might have on our comparison of spatial autocorrelation patterns. At Kingman, 21% of grid cells had 'no data' (81 out of 380). For the other islands, we assigned 'no data' values to grid cells at random until we reached the same ratio of missing data as Kingman, then repeated our moving window averaging process and recalculated the Moran's I statistic. We repeated this at each island 100 times, each time randomising the 'no data' grid cell locations. From the iterations, we calculated a mean re-sampled OMI and p-value and identified the smallest and largest scale at which $p \geq 0.05$ (see Supplementary material Appendix 1, Fig. A1).

## Results

### The spatial scaling of coral reef benthic communities across geographies

The spatial distribution of benthic functional groups appeared non-random around the circumference of each island, with some groups dominating large expanses of coastlines for several km (Fig. 1). On occasion, these regions of spatial dominance showed consistencies between islands. For example, macroalgae was spatially clumped along the southeast coast of Kingman and the south coast of neighbouring Palmyra, reaching 11 – 46% cover over a 1.8 km stretch of coastline at Kingman and 25 – 68% along a 1.5 km stretch at Palmyra (Fig. 1). Different coral morphologies also exhibited non-random distributions, and again displayed discrete zones of spatial dominance along coastlines (Fig. 1). For example, plating coral

peaked at 70% cover and dominated 1.2 km of Kingman's south coast, while branching coral cover dominated the northeast coast of neighbouring Howland and Baker for 1.1 km and 1.2 km, respectively (Fig.1).

All benthic functional groups displayed strong evidence of spatial clustering (positive autocorrelation) around the circumference of each island, but the scale and strength of this autocorrelation differed between islands (Fig. 2). Around Howland, crustose coralline algae (CCA) and turf algae showed positive spatial autocorrelation at scales up to 0.3 km and CCA had similar spatial clustering at neighbouring Baker. Around Kingman, Jarvis and Baker, turf algae were spatially clustered across the seascape at scales of ~1 km. Macroalgae and hard corals displayed comparable scaling patterns at neighbouring Howland and Baker; both groups were spatially clustered at scales up to ~500 m at Howland and ~1 km at Baker. These inter-island spatial autocorrelation patterns were robust to variations in the number and spatial distribution of grid cells containing no data; the scales at which benthic functional groups significantly differed from random only changed by up to 100 m (see Supplementary material Appendix 1, Fig. A1). Macroalgae were the most spatially clustered of any functional group at the finest resolution of our data (100 m), having a consistently high Observed Moran's I Index of ~0.4 around Baker, Kingman and Palmyra (Fig. 2). However, the spatial distribution of macroalgae at Jarvis did not differ from random at any scale, likely due to its low island-mean cover of 1.8% (almost 3 times lower than at Kingman, the island with the next lowest abundance).

Different coral morphologies also showed strong evidence of spatial clustering around the circumference of each island, with some consistencies in scaling between morphologies of the same type at different islands (Fig. 3). At neighbouring Howland and Baker, branching corals were spatially clustered up to scales of 700 – 800 m and followed a similar gradient in spatial autocorrelation across scales (Fig. 3). The scaling of encrusting corals was also similar

between Kingman, Howland and Palmyra, being spatially clustered up to scales of 1.1 – 1.3 km (Fig. 3). Branching corals at Howland and Baker and plating corals at Jarvis had their highest degree of spatial clustering at the finest spatial resolution (100 m) (Fig. 3). In contrast, plating corals at other islands, as well as submassive, corymbose and encrusting coral morphologies, peaked in autocorrelation at a 200 m scale, suggesting a less clustered distribution at smaller spatial scales (Fig. 3).

**Correlation between the spatial scaling properties of benthic communities and their physical drivers**

There were cases where the upper scale of significant spatial clustering remained similar between benthic community members and the physical drivers. At the functional group resolution, this overall correlation was stronger for wave energy ($\rho$= 0.73) than for subsurface temperature ($\rho$= 0.46) as well as individually for any single benthic functional group ($\rho$= 0.71 – 0.93 for wave energy, 0.37 – 0.82 for subsurface temperature) (Fig. 4) (see Supplementary material Appendix 1 Fig. A2 for spatial autocorrelation patterns in wave energy and subsurface temperature across scales). There was also inter-island variability in this alignment. For example, around Baker, wave energy was spatially clustered up to scales of ~1 km and turf algae, macroalgae and hard coral were also clustered up to ~1 km. Around Kingman, subsurface temperature and turf algae were both spatially clustered up to ~1 km, while wave energy and hard coral cover were both clustered up to scales of ~2.4 km. In contrast, there was consistently poor alignment at Palmyra, with none of the upper scales of significant autocorrelation in the benthic functional groups closely resembling those of the physical drivers (Fig. 4).

The correlation between the upper scale at which there remained significant spatial autocorrelation in the benthos and physical drivers was not as strong fohard coral

morphologies (ρ= 0.50 and 0.46 for wave energy and subsurface temperature, respectively). There was substantial variation across the different coral morphologies, with some showing closer alignment to the physical drivers than others. For example, the spatial scaling of plating corals closely matched those of wave energy regardless of island, and some coral morphologies appeared to be more closely aligned at specific islands than others (Fig. 5). Encrusting corals around Howland were spatially clustered up to 1.1 km, exactly matching the spatial scaling of subsurface temperature and wave energy. At Jarvis, plating corals were clustered up to 1.4 km, similar to the spatial clustering exhibited by both subsurface temperature and wave energy (to within 200 m). Finally, at Kingman, encrusting and submassive corals and subsurface temperature were spatially clustered up to scales of ~1 km, while plating corals and wave energy were both clustered up to ~2 km scales (Fig. 5).

## Discussion

### The autocorrelated nature of coral reef seascapes

Our results show that coral reef benthic communities are naturally spatially clustered across tropical island seascapes, with individual groups in some cases dominating entire km-sections of coastline (Fig. 1). Structural complexity of benthic assemblages can be influenced by the dominant functional group or coral morphology, which will have an effect on the spatial structure of reef-associated organisms, including fish communities (Alvarez-Filip et al. 2011, Richardson et al. 2017). Furthermore, these sections of dominance are evidence that 'ecotones'– discrete transition points between two communities or habitat types – exist around these tropical oceanic islands, which will likely have structuring effects on reef-associated organisms, akin to those of forest edges (Pfeifer et al. 2017) and coral reef-seagrass transition zones (Dorenbosch et al. 2005). Acknowledging the autocorrelated nature

of coral reef benthic communities, may have important management implications. For example, larger patches dominated by hard coral of a structurally complex morphology with a seagrass-hard coral ecotone, may be more beneficial to maintain ecosystem structure and function. Such patterns of naturally occurring spatial autocorrelation should be considered in marine spatial planning and coral restoration efforts that may attempt to mimic the inherent spatial properties of coral reefs.

The spatial scaling patterns of benthic groups differed across geographies but had the common attribute of displaying positive spatial autocorrelation up to several kilometres of scale across all five study islands. Previously, Bradbury and Young (1983) found corals to be spatially clumped at 60-m scales across shallow reef flats and reef crests of the Great Barrier Reef in Australia. Edwards et al. (2017) also found most coral taxa were spatially clustered within 100 $m^2$ plots at 10 m depth on the outer reef slope of Palmyra Atoll, central Pacific (one of our study islands). We found the highest levels of positive autocorrelation in all benthic community members at our smallest spatial scales (100 – 200 m) around all five of our study islands. We therefore hypothesise that positive autocorrelation, particularly at smaller scales, is a common spatial attribute of corals and other benthic organisms across depths, reef habitats, and geographies.

**Drivers of coral reef benthic community seascapes**

The non-random spatial dominance of benthic functional groups and hard coral morphologies around kilometre-sections of our five study islands likely exist, in part, because of concurrent gradients in the physical environment. Physical environmental drivers are key determinants of benthic community structure around oceanic islands, promoting or limiting the abundance of competitors particularly in the absence of local human impacts (Gove et al. 2015, Williams et al. 2015a). Howland, Baker and Jarvis have pronounced cross-island

gradients in subsurface temperature, reflective of localised upwelling along their western coasts that results in the up-slope movement of deep, cold, nutrient-rich waters onto shallow reef communities (Gove et al. 2006, Tsuda et al. 2008, Aston et al. 2019). Algae can benefit from increased growth under high nutrient conditions on coral reefs (Littler et al. 1983, Miller et al. 1999), which may explain spatial clustering of turf algae and macroalgae along continuous km-scale sections of Baker and Howland's western coasts, respectively. As well as benefiting algae, upwelling can enhance growth rates in reef-building corals (Diaz-Pulido and Garzón-Ferreira 2002, Edmunds and Leichter 2016) by providing heterotrophic energetic subsidies (Williams et al. 2018). In some cases, this can give corals a competitive advantage over algae and strong upwelling is thought to explain the kilometre-sections of hard coral dominance along the western coast of Jarvis (Aston et al. 2019).

Like competing benthic functional groups, individual hard coral morphologies displayed strong spatial clustering along kilometre-sections of the island coastlines that are also likely driven, in part, by gradients in physical drivers. Our results indicate that the high spatial clustering of hard coral along the western coast of Jarvis, a more wave-sheltered part of the island, is almost exclusively dominated by plating coral. Plating and branching corals are susceptible to breakage and dislodgement by high wave energy (Madin et al. 2014), whereas encrusting, digitate and massive coral morphologies are more wave-resistant and dominate in more wave-exposed areas (Gove et al. 2015). Branching corals also dominated sections of Howland and Baker's north-eastern to south-eastern coasts, which are sheltered from winter storm swells from the north-west (Mundy et al. 2010). In contrast, Palmyra's northern coast is exposed to north-west winter swells (Williams et al. 2013) and here we saw spatial clustering of more wave-tolerant encrusting and corymbose corals.

Benthic functional groups not only dominated km-sections of island coastlines, but also showed non-random patterns of spatial clustering across scales (Fig. 2, 3). In some cases,

375 the upper scale at which benthic functional groups were spatially clustered around islands
376 closely correlated with the upper scale at which the physical drivers were spatially clustered
377 (Fig. 4). This correlation was more evident with wave energy than subsurface temperature
378 regardless of functional group, and across functional groups, the strongest correlations with
379 the physical drivers were evident in turf algae and CCA. High wave energy often favours
380 low-lying, wave-tolerant algae, such as turf and CCA and limits the dominance of larger
381 upright macroalgae that, like some corals, are vulnerable to dislodgement (Page-Albins et al.
382 2012, Williams et al. 2013, Gove et al. 2015). Our findings show, for the first time, that
383 physical drivers on coral reefs not only limit or promote the abundance of individual benthic
384 groups, but also play a key role in governing their spatial scaling properties across tropical
385 seascapes.

386 The spatial scaling of coral reef benthic communities was more similar between
387 islands closer in proximity and size. For example, at neighbouring Kingman and Palmyra (63
388 km apart), macroalgae were spatially structured up to ~3 km scales at both islands. At
389 neighbouring Howland and Baker (69 km apart), CCA was spatially structured up to scales of
390 0.3 km at both islands. We hypothesise that these common benthic scaling patterns between
391 closely situated islands reflect broader-scale autocorrelation in environmental conditions that
392 exist across archipelagos, with islands in closer proximity exposed to similar surrounding
393 environmental conditions (Gove et al. 2013). Kingman and Palmyra also have much larger
394 total reef areas and longer coastlines, producing more expansive areas of reef slope of the
395 same aspect, than at the other three islands (Gove et al. 2016). This may allow environmental
396 homogeneity over greater linear extents, particularly with regards to incoming wave energy
397 and could give rise to the large homogeneous zones of spatial dominance by single benthic
398 functional groups and coral morphologies that we observe at Kingman and Palmyra. Smaller

399 coastlines and total reef areas at Howland, Baker and Jarvis could explain why benthic
400 functional groups here, only remained spatially clustered at smaller spatial scales.
401 Our results support the expectation that environmental drivers can cause ecological
402 responses at larger spatial scales, while biotic factors drive smaller-scale patterns and
403 processes (Legendre 1993). We found the upper bounds in scale at which the benthic and
404 physical variables showed spatial clustering were highly correlated, suggesting that physical
405 drivers set the upper spatial bound in which benthic communities are spatially organised
406 around tropical oceanic islands. At smaller spatial scales (100 – 200 m), we saw the highest
407 degree of benthic community spatial clustering, which may be better explained by biotic
408 factors. For example, the dominant macroalgae around our study islands are calcifying
409 *Halimeda* (Vroom et al. 2010, Williams et al. 2013) that reproduce asexually over short
410 distances by fragmentation. This type of reproduction could explain the high degrees of
411 macroalgal spatial clustering at scales of 100 – 200 m around Kingman, Palmyra, Howland
412 and Baker. Similarly, the high spatial clustering of branching corals at smaller scales at
413 Howland and Baker, could be explained by the branching corals all being fast-growing
414 Acroporids that can also reproduce over short distances through fragmentation (Baird and
415 Hughes 2000).
416
417 **Conclusion**
418 For the first time, we quantify the autocorrelated nature of coral reef seascapes across
419 geographies in the absence of direct local human impacts. All major benthic functional
420 groups and hard coral morphologies showed evidence of positive autocorrelation (spatial
421 clustering) up to scales of 0.3 to 3.5 km around the circumference of five oceanic tropical
422 islands. The scales across which benthic community members exhibited spatial structure and
423 the strength of these autocorrelation patterns differed between islands but was more similar

between islands closer in proximity and of a similar size. In some cases, benthic community spatial scaling was similar to the scaling of concurrent gradients in physical drivers, in particular wave energy. This suggests that physical drivers not only play a role in governing patterns of community abundance on tropical coral reefs, but also contribute to determining their spatial scaling properties across the seascape. How these patterns of biological autocorrelation change in response to changes in physical gradients, such as those that occur during environmental disturbance events, remains unknown and is an exciting avenue for future research.

**Acknowledgements**

We thank NOAA's Pacific Islands Fisheries Science Center (PIFSC) Ecosystem Sciences Division and the officers and crews of the NOAA ships Hi'ialakai and Oscar Elton Sette for coordinating and conducting all towed-diver surveys. HVF was supported by a Envision Doctoral Training Programme scholarship funded by the National Environment Research Council (NERC) of the U.K. and co-funding from The Nature Conservancy. We thank members of the Reef Systems Lab at Bangor University's School of Ocean Sciences for their collective advice towards project development, the NOAA internal review process and two anonymous reviewers for their helpful comments on the manuscript draft, and Amanda Dillon at Aline Design for help with figure formatting.

Author contributions – HVF and GJW conceived the study; HVF analysed the data with GJW, JMG and AJD; HVF wrote the manuscript with GJW. All authors contributed to the editing of the manuscript.

# References


Addicott, J. F. et al. 1987. Ecological Neighborhoods: Scaling Environmental Patterns. - Oikos 49: 340.

Alvarez-Filip, L. et al. 2011. Complex reef architecture supports more small-bodied fishes and longer food chains on Caribbean reefs. - Ecosphere 2: 1–17.

Aston, E. A. et al. 2019. Scale-dependent spatial patterns in benthic communities around a tropical island seascape. - Ecography. 42: 578–590.

Baird, A. H. and Hughes, T. P. 2000. Competitive dominance by tabular corals: an experimental analysis of recruitment and survival of understorey assemblages. - J. Exp. Mar. Bio. Ecol. 251: 117–132.

Beijbom, O. et al. 2015. Towards Automated Annotation of Benthic Survey Images: Variability of Human Experts and Operational Modes of Automation. - PLoS One 10: e0130312.

Boström, C. et al. 2011. Seascape ecology of coastal biogenic habitats: advances, gaps, and challenges. - Mar. Ecol. Prog. Ser. 427: 191–217.

Bradbury, R. and Young, P. 1983. Coral interactions and community structure: an analysis of spatial pattern. - Mar. Ecol. Prog. Ser. 11: 265–271.

Cocu, N. et al. 2005. Spatial autocorrelation as a tool for identifying the geographical patterns of aphid annual abundance. - Agric. For. Entomol. 7: 31–43.

D'Urban Jackson, T. et al. 2020. Three-dimensional digital mapping of ecosystems: a new era in spatial ecology. - Proc. R. Soc. B Biol. Sci. 287: 20192383.

De Knegt, H. J. et al. 2011. The spatial scaling of habitat selection by African elephants. - J. Anim. Ecol. 80: 270–281.

Diaz-Pulido, G. and Garzón-Ferreira, J. 2002. Seasonality in algal assemblages on upwelling-influenced coral reefs in the Colombian Caribbean. - Bot. Mar. 45: 284–292.

474 Dorenbosch, M. et al. 2005. Distribution of coral reef fishes along a coral reef-seagrass
475 gradient: Edge effects and habitat segregation. - Mar. Ecol. Prog. Ser. 299: 277–288.
476 Dungan, J. L. et al. 2002. A balanced view of scale in spatial statistical analysis. - Ecography.
477 25: 626–640.
478 Edmunds, P. J. and Leichter, J. J. 2016. Spatial scale-dependent vertical zonation of coral reef
479 community structure in French Polynesia. - Ecosphere 7: e01342.
480 Edwards, C. B. et al. 2017. Large-area imaging reveals biologically driven non-random
481 spatial patterns of corals at a remote reef. - Coral Reefs. 36: 1291-1305
482 Estes, L. et al. 2018. The spatial and temporal domains of modern ecology. - Nat. Ecol. Evol.
483 2: 819–826.
484 Fortin, M.-J. et al. 2016. Spatial Analysis in Ecology. - In: Wiley StatsRef: Statistics
485 Reference Online. John Wiley & Sons, Ltd, pp. 1–13.
486 Gobbi, M. and Brambilla, M. 2016. Patterns of spatial autocorrelation in the distribution and
487 diversity of carabid beetles and spiders along Alpine glacier forelands. - Ital. J. Zool. 83:
488 600–605.
489 Gove, J. M. et al. 2006. Temporal variability of current-driven upwelling at Jarvis Island. - J.
490 Geophys. Res. 111: C12011.
491 Gove, J. M. et al. 2013. Quantifying Climatological Ranges and Anomalies for Pacific Coral
492 Reef Ecosystems. - PLoS One 8: e61974.
493 Gove, J. M. et al. 2015. Coral reef benthic regimes exhibit non-linear threshold responses to
494 natural physical drivers. 522: 33–48.
495 Gove, J. M. et al. 2016. Near-island biological hotspots in barren ocean basins. - Nat.
496 Commun. 7: 1–8.
497 Hamylton, S. M. and Barnes, R. S. K. 2018. The effect of sampling effort on spatial
498 autocorrelation in macrobenthic intertidal invertebrates. - Hydrobiologia 811: 239–250.

499 Hatcher, B. G. et al. 1987. Scaling analysis of coral reef systems: an approach to problems of
500 scale. - Coral Reefs 5: 171–181.
501 Heenan, A. et al. 2020. Natural variation in coral reef trophic structure across environmental
502 gradients. - Front. Ecol. Environ. 18: 69–75.
503 Hinchey, E. K. et al. 2008. Preface: Marine and coastal applications in landscape ecology. -
504 Landsc. Ecol. 23: 1–5.
505 Hochberg, E. J. and Atkinson, M. J. 2003. Capabilities of remote sensors to classify coral,
506 algae, and sand as pure and mixed spectra. - Remote Sens. Environ. 85: 174–189.
507 Hughes, T. P. et al. 2017. Coral reefs in the Anthropocene. - Nature 546: 82–90.
508 Jones, K. B. et al. 2013. Informing landscape planning and design for sustaining ecosystem
509 services from existing spatial patterns and knowledge. - Landsc. Ecol. 28: 1175–1192.
510 Kenny, A. et al. 2003. An overview of seabed-mapping technologies in the context of marine
511 habitat classification. - ICES J. Mar. Sci. 60: 411–418.
512 Kenyon, J. C. et al. 2006. Towed-Diver Surveys, a Method for Mesoscale Spatial Assessment
513 of Benthic Reef Habitat: A Case Study at Midway Atoll in the Hawaiian Archipelago. -
514 Coast. Manag. 34: 339–349.
515 Lee, M. F. et al. 2008. Remote sensing assessment of forest damage in relation to the 1996
516 strong typhoon Herb at Lienhuachi Experimental Forest, Taiwan. - For. Ecol. Manage.
517 255: 3297–3306.
518 Legendre, P. 1993. Spatial Autocorrelation: Trouble or New Paradigm? - Ecology 74: 1659–
519 1673.
520 Levin, S. A. 1992. The Problem of Pattern and Scale in Ecology: The Robert H. MacArthur
521 Award Lecture. - Ecology 73: 1943–1967.
522 Levy, J. et al. 2018. Assessing the spatial distribution of coral bleaching using small
523 unmanned aerial systems. - Coral Reefs 37: 373–387.

524 Littler, M. M. et al. 1983. Evolutionary strategies in a tropical barrier reef system:
525 Functional-form groups of marine macroalgae. - J. Phycol. 19: 229–237.
526 Madin, J. S. et al. 2014. Mechanical vulnerability explains size-dependent mortality of reef
527 corals. - Ecol. Lett. 17: 1008–1015.
528 Miller, M. W. et al. 1999. Effects of nutrients versus herbivores on reef algae: A new method
529 for manipulating nutrients on coral reefs. - Limnol. Oceanogr. 44: 1847–1861.
530 Moran, P. A. P. 1950. Notes on Continuous Stochastic Phenomena. - Biometrika 37: 17.
531 Mumby, P. J. et al. 1997. Coral reef habitat-mapping: How much detail can remote sensing
532 provide? - Mar. Biol. 130: 193–202.
533 Mundy, B. C. et al. 2010. Inshore Fishes of Howland Island, Baker Island, Jarvis Island,
534 Palmyra Atoll, and Kingman Reef. - Atoll Res. Bull. 585
535 Murdoch, T. J. T. and Aronson, R. B. 1999. Scale-dependent spatial variability of coral
536 assemblages along the Florida Reef Tract. - Coral Reefs 18: 341–351.
537 Nash, K. L. et al. 2014. Discontinuities, cross-scale patterns, and the organization of
538 ecosystems. - Ecology 95: 654–667.
539 Norström, A. V et al. 2016. Guiding coral reef futures in the Anthropocene. - Front. Ecol.
540 Environ. 14: 490–498.
541 Page-Albins, K. N. et al. 2012. Patterns in Benthic Coral Reef Communities at Pearl and
542 Hermes Atoll along a Wave-Exposure Gradient. - Pacific Sci. 66: 481–496.
543 Pedersen, N. E. et al. 2019. The influence of habitat and adults on the spatial distribution of
544 juvenile corals. - Ecography. 42: 1703–1713.
545 Pfeifer, M. et al. 2017. Creation of forest edges has a global impact on forest vertebrates. -
546 Nature 551: 187–191.
547 Pittman, S. J. et al. 2011. Practicing coastal seascape ecology. - Mar. Ecol. Prog. Ser. 427:
548 187–190.

549 Purkis, S. J. 2018. Remote Sensing Tropical Coral Reefs: The View from Above. - Ann. Rev.
550 Mar. Sci. 10: 149–168.
551 R Core Team 2019. R: A laguage and environment for statistical computing.
552 Rahbek, C. and Graves, G. R. 2000. Detection of macro-ecological patterns in South
553 American hummingbirds is affected by spatial scale. - Proc. R. Soc. B Biol. Sci. 267:
554 2259–2265.
555 Richardson, L. E. et al. 2017. Structural complexity mediates functional structure of reef fish
556 assemblages among coral habitats. - Environ. Biol. Fishes 100: 193–207.
557 Schneider, D. C. 1994. Quantitative Ecology: Spatial and Temporal Scaling. - Elsevier.
558 Schneider, D. C. 2001. The rise of the concept of scale in ecology. - Bioscience 51: 545–553.
559 Tsuda, R. T. et al. 2008. Additional Marine Benthic Algae from Howland and Baker Islands,
560 Central Pacific 1. - Pacific Sci. 62: 271–290.
561 Vargas-Ángel, B. et al. 2011. Severe, Widespread El Niño–Associated Coral Bleaching in the
562 US Phoenix Islands. - Bull. Mar. Sci. 87: 623–638.
563 Vroom, P. S. et al. 2010. Marine biological community baselines in unimpacted tropical
564 ecosystems: Spatial and temporal analysis of reefs at Howland and Baker Islands. -
565 Biodivers. Conserv. 19: 797–812.
566 Wagner, H. H. and Fortin, M.-J. 2005. Spatial analysis of landscapes: concepts and statistics.
567 - Ecology 86: 1975–1987.
568 Wedding, L. M. et al. 2011. Quantifying seascape structure: Extending terrestrial spatial
569 pattern metrics to the marine realm. - Mar. Ecol. Prog. Ser. 427: 219–232.
570 Wiens, J. A. and Milne, B. T. 1989. Scaling of “landscapes” in landscape ecology, or,
571 landscape ecology from a beetle’s perspective. - Landsc. Ecol. 3: 87–96.
572 Williams, G. J. et al. 2010. Modeling patterns of coral bleaching at a remote Central Pacific
573 atoll. - Mar. Pollut. Bull. 60: 1467–1476.

Williams, G. J. et al. 2013. Benthic communities at two remote pacific coral reefs: Effects of reef habitat, depth, and wave energy gradients on spatial patterns. - PeerJ 2013: 1–26.

Williams, G. J. et al. 2015a. Local human impacts decouple natural biophysical relationships on Pacific coral reefs. - Ecography. 38: 751–761.

Williams, S. M. et al. 2015b. Hierarchical spatial patterns in Caribbean reef benthic assemblages. - J. Biogeogr. 42: 1327–1335.

Williams, G. J. et al. 2018. Biophysical drivers of coral trophic depth zonation. - Mar. Biol. 165: 60.

Williams, G. J. et al. 2019. Coral reef ecology in the Anthropocene. - Funct. Ecol. 33: 1014–1022.

Zhang, N. and Zhang, H. 2011. Scale variance analysis coupled with Moran's *I* scalogram to identify hierarchy and characteristic scale. - Int. J. Geogr. Inf. Sci. 25: 1525–1543.

Zhang, X. et al. 2009. NDVI spatial pattern and its differentiation on the Mongolian Plateau. - J. Geogr. Sci. 19: 403–415.

## Figure captions

**Figure 1.** Spatial variations in percentage cover of coral reef benthic functional groups and dominant hard coral morphologies on the outer reef slopes (~15 m depth) of five uninhabited central Pacific islands collected via towed-diver digital image surveys in 2008 across ~140 linear km of reef (n = 6022 images). The white cells around each island are 100-m grid cells that overlap the towed-diver tracks and are used to spatially reference individual images (their numbers start due north and correspond with those on the island rosette plots). Grey regions on the rosette plots represent missing data regions. The islands are ordered in increasing size top to bottom.

**Figure 2.** Patterns of spatial autocorrelation (solid coloured line) in the percentage cover of benthic functional groups at increasing 100-m scale increments around five uninhabited central Pacific islands. The Observed Moran's I (OMI) value indicates a clustered distribution (+ve values), random distribution (0 value, horizontal dotted line) to increasingly dispersed (-ve values). The OMI is calculated for all possible starting points around each island and the range in these values for each scale is shown as the shaded region. The vertical dotted line shows the scale at which the OMI value is not significantly different from random for each benthic group ($p \geq 0.05$). CCA, crustose coralline algae.

**Figure 3.** Patterns of spatial autocorrelation (solid coloured line) in the percentage cover of dominant hard coral morphologies at increasing 100-m scale increments around five uninhabited central Pacific islands. The Observed Moran's I (OMI) value indicates a clustered distribution (+ve values), random distribution (0 value, horizontal dotted line) to increasingly dispersed (-ve values). The OMI is calculated for all possible starting points around each island and the range in these values for each scale is shown as the shaded region. The vertical dotted line shows the scale at which the OMI value is not significantly different from random for each benthic group ($p \geq 0.05$).

**Figure 4.** Correlation between the upper scale at which there remained significant spatial clustering in the benthic functional groups and physical drivers around five uninhabited central Pacific islands (diagonal dotted line is a 1:1 reference). Overall Spearman Rank correlation coefficient ($\rho$) equaled 0.73 for wave energy and 0.46 for subsurface temperature. Correlation values for each individual benthic functional group and wave energy equaled: crustose coralline algae (CCA) = 0.81, turf algae = 0.93, hard coral = 0.71, macroalgae =

624 0.79), and for subsurface temperature equaled: CCA = 0.48, turf algae = 0.82, hard coral =
625 0.37, macroalgae = 0.47).
626
627 **Figure 5.** Correlation between the upper scale at which there remained significant spatial
628 clustering in the dominant hard coral morphologies and physical drivers around five
629 uninhabited central Pacific islands (diagonal dotted line is a 1:1 reference). Overall Spearman
630 Rank correlation coefficient (ρ) equaled 0.50 for wave energy and 0.46 for subsurface
631 temperature. Note that unlike in Fig. 4, correlation values for individual morphologies are not
632 calculated due to a lack of adequate replication across islands.
633
634

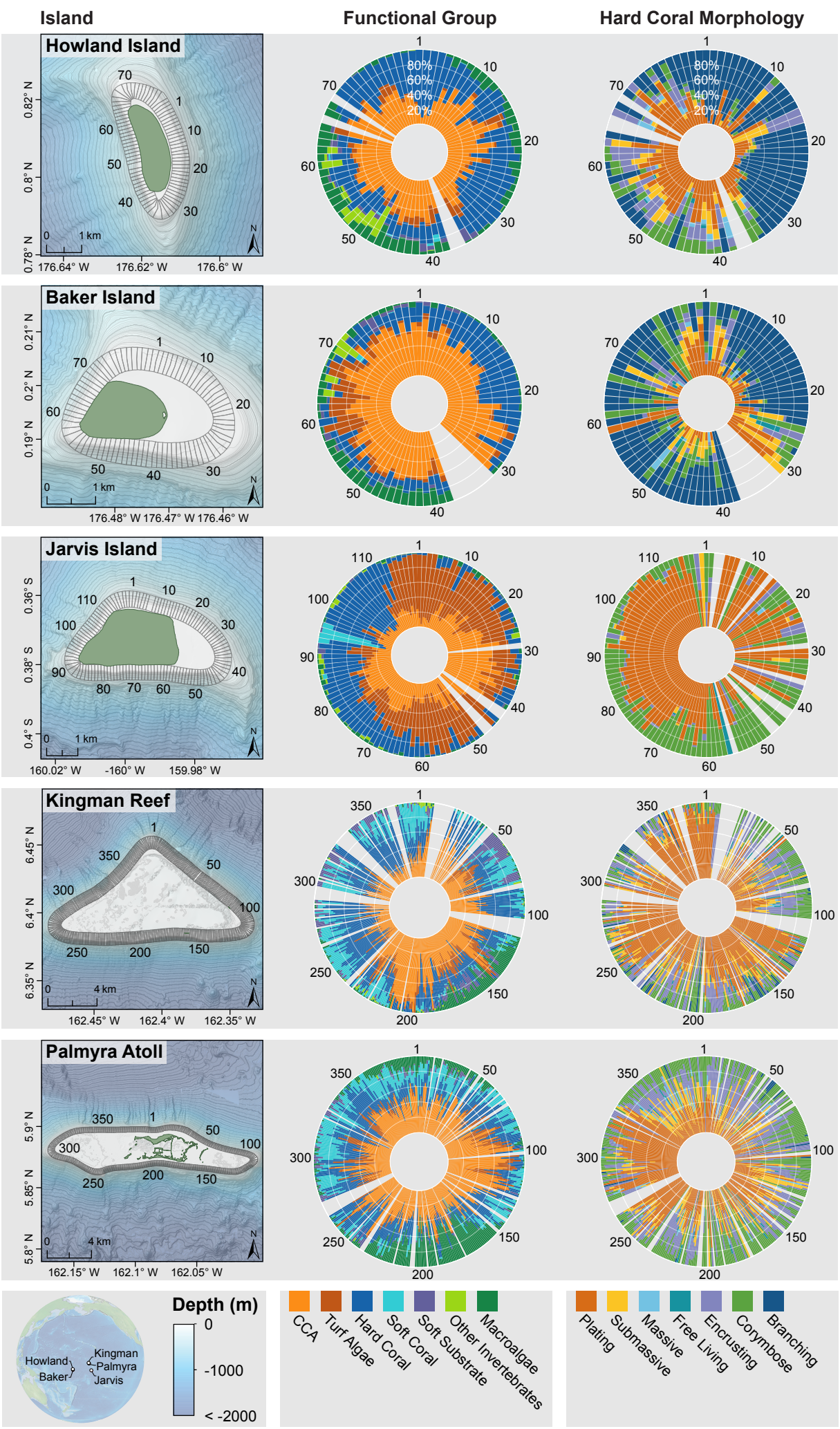
Island
Functional Group
Hard Coral Morphology
Howland Island
0.82° N
0.8° N
0.78° N
176.64° W
176.62° W
176.6° W
0
1 km
N
Baker Island
0.21° N
0.2° N
0.19° N
176.48° W
176.47° W
176.46° W
Jarvis Island
0.36° S
0.38° S
0.4° S
160.02° W
-160° W
159.98° W
Kingman Reef
6.45° N
6.4° N
6.35° N
162.45° W
162.4° W
162.35° W
4 km
Palmyra Atoll
5.9° N
5.85° N
5.8° N
162.15° W
162.1° W
162.05° W
80%
60%
40%
20%
Howland
Baker
Kingman
Palmyra
Jarvis
Depth (m)
0
-1000
< -2000
CCA
Turf Algae
Hard Coral
Soft Coral
Soft Substrate
Other Invertebrates
Macroalgae
Plating
Submassive
Massive
Free Living
Encrusting
Corymbose
Branching

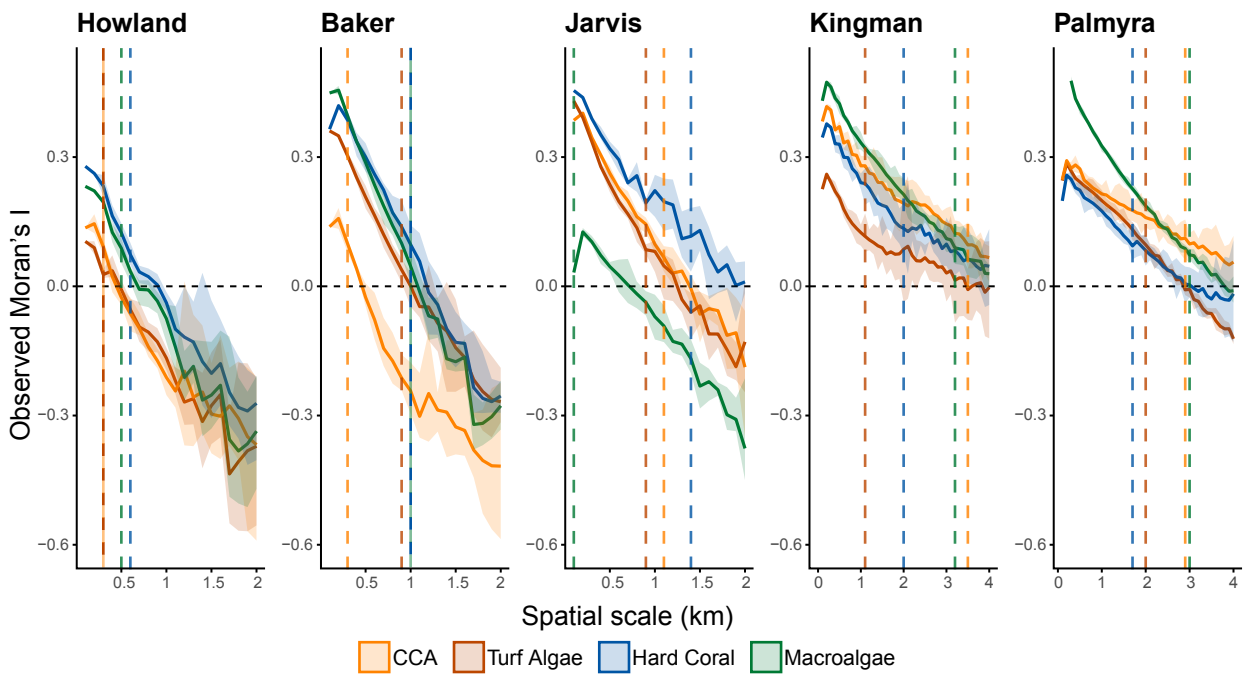
Howland
Baker
Jarvis
Kingman
Palmyra
Observed Moran's I
0.3
0.0
−0.3
−0.6
0.5
1
1.5
2
0
1
2
3
4
Spatial scale (km)
CCA
Turf Algae
Hard Coral
Macroalgae

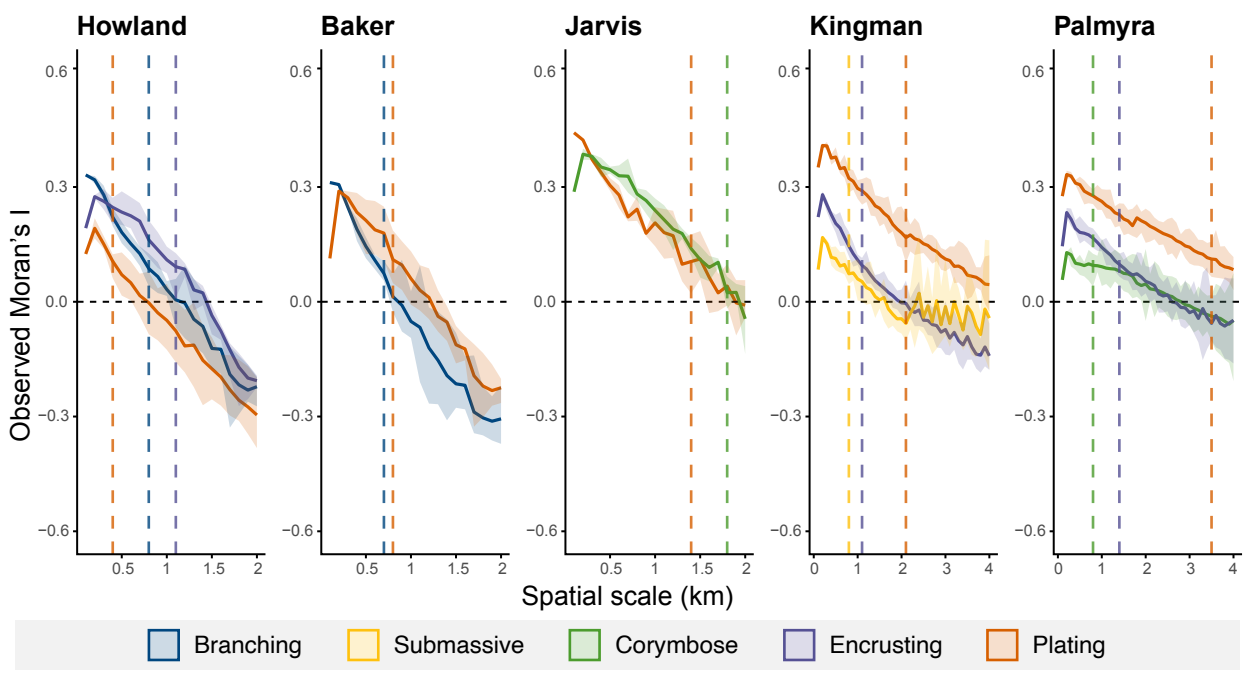
Howland
Baker
Jarvis
Kingman
Palmyra
Observed Moran's I
Spatial scale (km)
Branching
Submassive
Corymbose
Encrusting
Plating

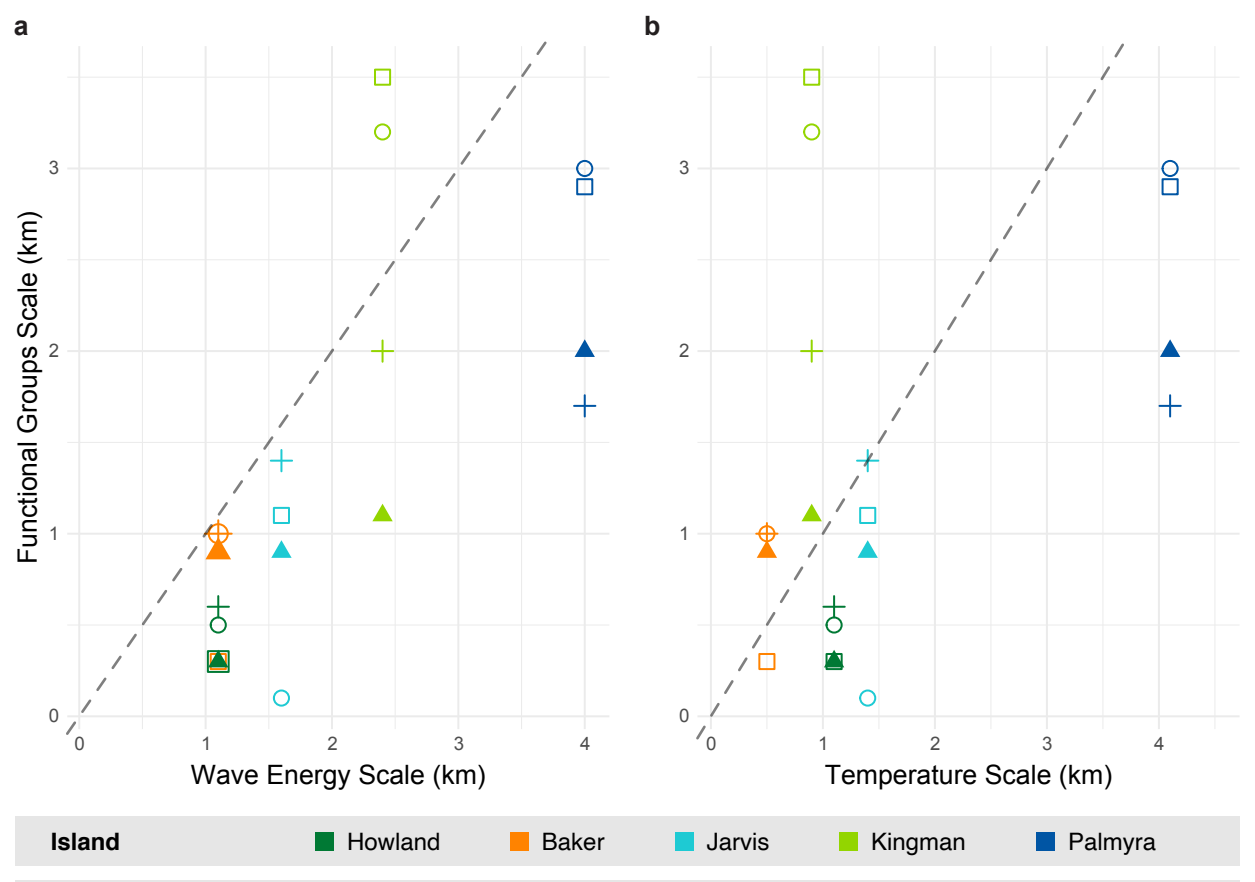
a
b
Functional Groups Scale (km)
Wave Energy Scale (km)
Temperature Scale (km)
0
1
2
3
4
Island
Howland
Baker
Jarvis
Kingman
Palmyra
Functional Group
CCA
Hard coral
Macroalgae
Turf

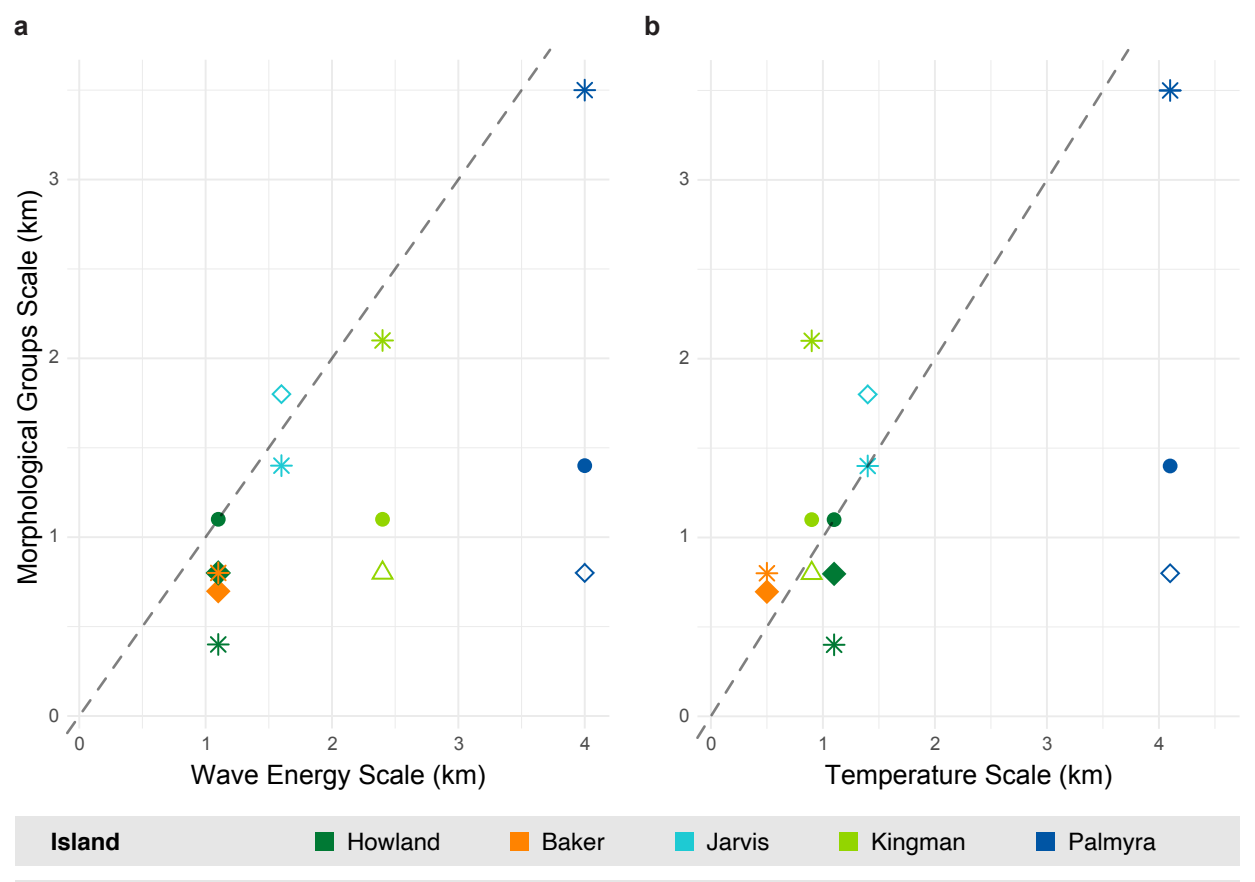
a
b
Morphological Groups Scale (km)
Wave Energy Scale (km)
Temperature Scale (km)
0
1
2
3
4
Island
Howland
Baker
Jarvis
Kingman
Palmyra
Morphology
Branching
Submassive
Corymbose
Encrusting
Plating

**Supplementary Material: Appendix 1**

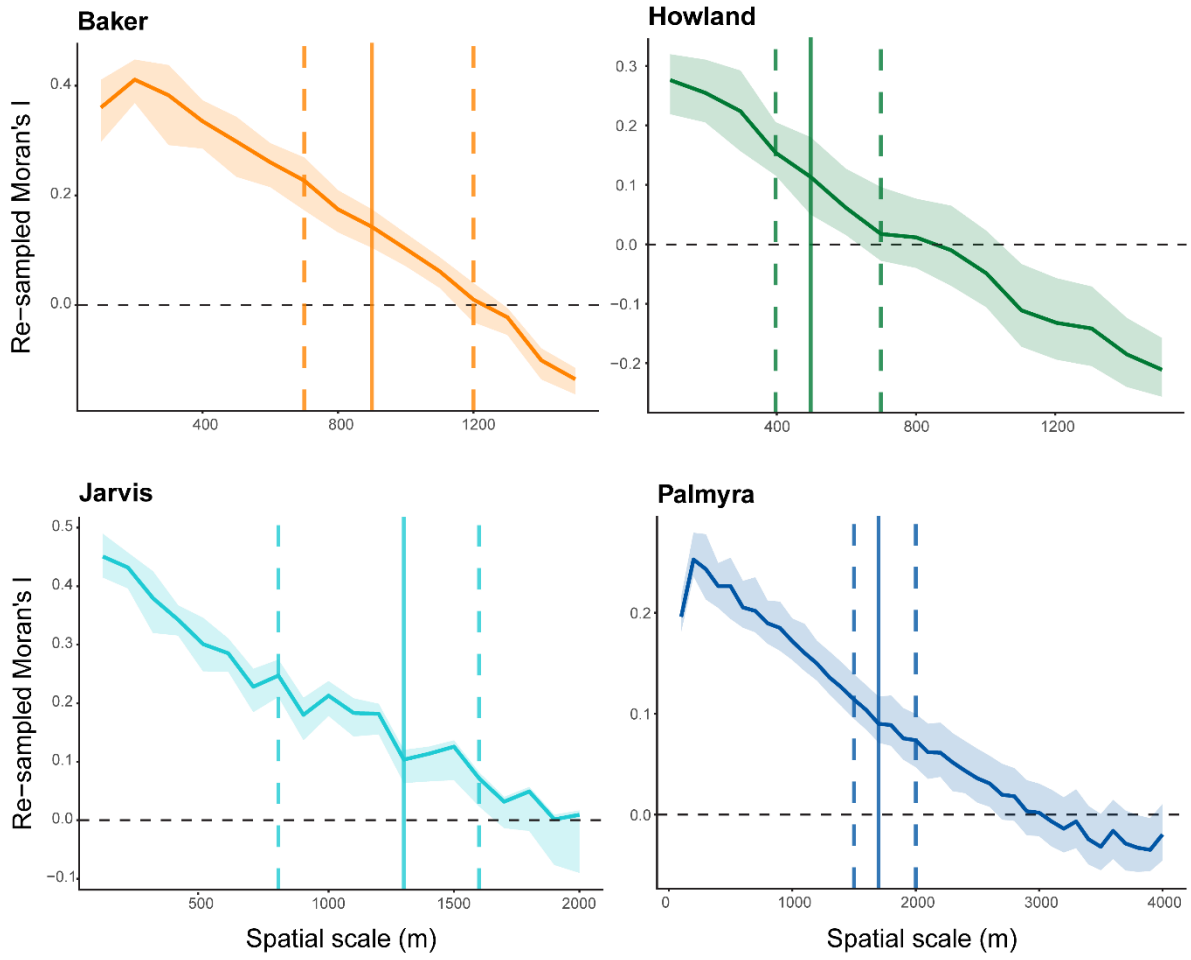


**Figure A1.** Sensitivity of Moran's I analysis to the number of island grid cells containing 'no data' (NA). The Moran's I analysis for hard coral percentage cover data was run 100 times with the same proportion of NA grid cells as Kingman (the island with the highest proportion of NA grid cells). NA grid cells were randomly distributed around the island each time the analysis was run. The result is a re-sampled Observed Moran's I (OMI) value across 100-m increment scales (solid coloured line) and the range in scale at which the OMI value is not significantly different from random ($p \geq 0.05$) (vertical dotted lines) and the mean scale across all 100 iterations (vertical solid line).

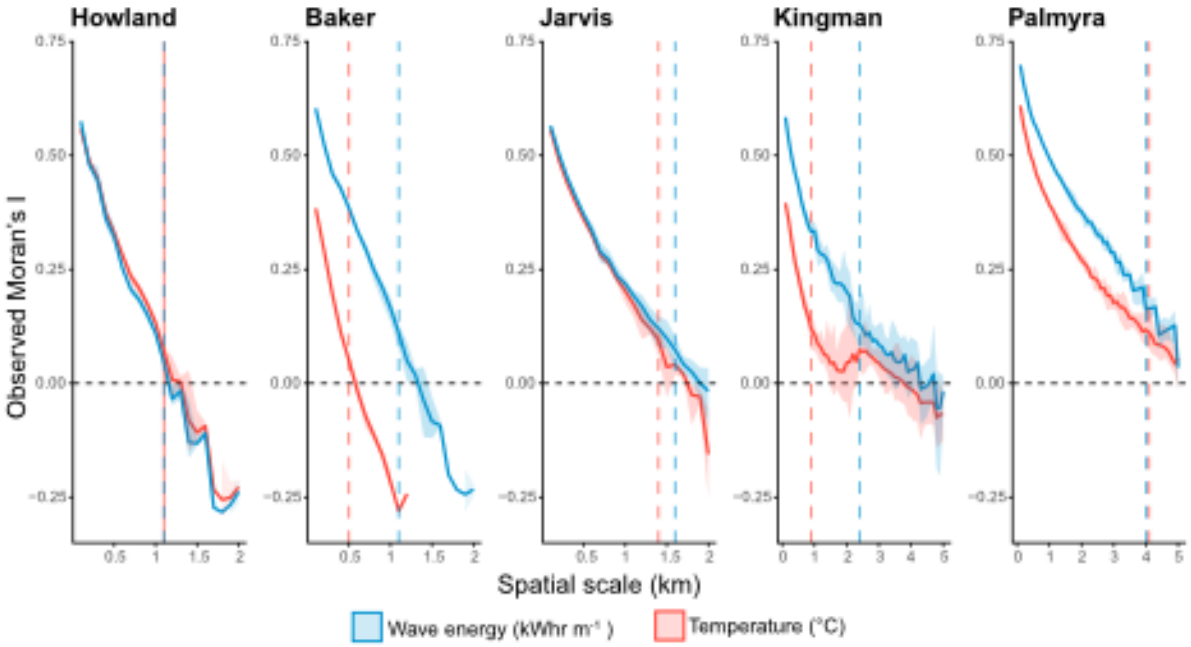


**Figure A2.** Patterns of spatial autocorrelation (solid coloured line) in surface wave energy (kW hr $m^{-1}$) and subsurface temperature (˚C) at 100-m scale increments around five uninhabited central Pacific islands. The Observed Moran's I (OMI) value indicates a clustered distribution (+ve values), random distribution (0 value, horizontal dotted line) to increasingly dispersed (-ve values). The OMI is calculated for all possible starting points around each island and the range in these values for each scale is shown as the shaded region. The vertical dotted line shows the scale at which the OMI value is not significantly different from random for each benthic group ($p \geq 0.05$).

**Table A1.** Benthic functional group definitions used during our benthic identification process and their source.

| **Functional Groups** | **Description** | **Based on source:** |
|---|---|---|
| **Hard Coral** | All Scleractinia | (Veron 2000) |
| **CCA** | Coraline Crustose Algae. Includes substrate and rubble covered in CCA. Also includes *Peyssonnelia* spp. which are functionally similar. | (Based on NOAA's PIFSC benthic image analysis classification scheme) |
| **Turf Algae** | Mixture of short often indistinguishable Algae. Including the "epilithic algal matrix" and defined as a mixed community of filamentous algae and cyanobacteria generally < 2 cm tall Often appearing as fuzzy carpets. On hard surfaces, as well as rubble and sand. | (Based on NOAA's PIFSC benthic image analysis classification scheme) |
| **Macroalgae** | Macroalgae or "fleshy" algae that are visible to the naked eye (typically >2cm) with evident structure and do not form crusts that adhere to rubble or substrate. | (Based on NOAA's PIFSC benthic image analysis classification scheme) |
| **Soft Coral** | All Alcyonacea | (Fabricius et al. 2001) |
| **Other Invertebrates** | Includes Anenomes, Echinoderms, Fire coral, Holothurians and other invertebrates that are not included in other categories. | (Williams et al. 2013) |
| **Soft Substrate** | Soft substrate is sand which is unconsolidated sediment ranging in texture and size from fine to coarse. Assigned to areas clearly distinguished as sand generally >1cm deep and without anything clearly growing on top. | (Based on NOAA's PIFSC benthic image analysis classification scheme) |

**Table A2.** Descriptions for each hard coral morphology within our benthic images and the source. Drawings by HVF.

| **Hard Coral Morphology** | **Description** | **Based on source:** | **Grouping for this study** |
|---|---|---|---|
| Branching  | Corals that branch and have secondary branches. | (Veron 2000) | Branching |
| Corymbose 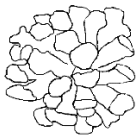 | Corals with a bush-like structure and closely arranged branches. | | Corymbose |
| Digitate  | Corals with finger-like upward projection. Grouped with corymbose as would have a similar level of vulnerability to wave action. | (Veron 2000) | Corymbose |
| Submassive  | Often an encrusting coral with irregular projections, or a short columnar appearance. Does not have similar size in all dimensions unlike massive corals. | | Submassive |
| Columnar  | Corals with vertical projections or forming columns. The projections take up more space vertically than horizontally. Grouped with Submassive as have similar structure and level of vulnerability to wave action. | (Veron 2000) | Submassive |
| Massive | | (Veron 2000) | Massive |

| | | | |
|---|---|---|---|
|  | Boulder-like or dome shaped corals with similar shape in all dimensions. | | |
| Free-living  | Corals that live unattached from the substrate. Often disk-shaped with a central mouth. | (Swanson et al. 2018) | Free-living |
| Plating  | The colony forms a plate-like structure that lifts off the surface of the substrate. | (Swanson et al. 2018) | Plating |
| Foliose  | Upright plates, often in whorls. Grouped with plating due to similarities in structure. | (Swanson et al. 2018) | Plating |
| Tabular 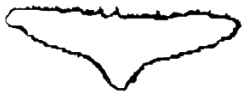 | Corals with a table like structure, with fused branches. May have had a central stalk attached to the substrate but this may be unseen by the angle of photos. If the coral is partly encrusting, classify as tabular. In this study, grouped together with Plating due to similarities in structure. | (Swanson et al. 2018) | Plating |
| Encrusting  | Vast majority of the coral adhered closely to the surface if not fully. Allowed for a one or two small abnormalities or projections. However, if numerous fragile projections were present, classified as submassive. | (Swanson et al. 2018) | Encrusting |

**Table A3.** Number of grid cells with 4 or more photos, compared to the total and as a percentage for each island.

| Island | Grid cells with ≥ 4 photos | Total grid cells | Percentage of grid cells with ≥ 4 photos |
|---|---|---|---|
| Jarvis | 114 | 119 | 95.8 |
| Palmyra | 340 | 394 | 86.3 |
| Kingman | 299 | 380 | 78.7 |
| Baker | 76 | 82 | 92.7 |
| Howland | 77 | 83 | 92.8 |